# 行政院國家科學委員會專題研究計畫 成果報告

## 二硫化鉬/金固體潤滑膜之磨潤特性研究
## 研究成果報告(精簡版)

計 畫 類 別 ：個別型
計 畫 編 號 ：NSC 99-2221-E-216-004-
執 行 期 間 ：99 年 08 月 01 日至 100 年 09 月 30 日
執 行 單 位 ：中華大學機械與航太工程研究所

計 畫 主 持 人：簡錫新
共 同 主 持 人：馬廣仁
計畫參與人員：碩士班研究生-兼任助理人員：吳崧銓
碩士班研究生-兼任助理人員：劉時瑞

報 告 附 件 ：國外研究心得報告

公 開 資 訊 ：本計畫可公開查詢

中 華 民 國 100 年 12 月 26 日

中 文 摘 要 ： 本研究將嘗試在二硫化鉬薄膜上鍍很薄的金膜層(約 80 nm)來更進一步增進二硫化鉬薄膜之使用其壽命。研究結果顯示很薄的金膜在最外層，做磨耗試驗時應力傳遞到二硫化鉬膜層，使得非晶態二硫化鉬轉變為層狀二硫化鉬，因此具有極低的摩擦係數，因為金的存在可改善二硫化鉬氧化現象，因此長時間的磨耗試驗仍可使二硫化鉬/金複合膜層維持很低的摩擦係數，二硫化鉬之使用壽命也因此大幅提升。氮化鈦硬膜上施鍍軟的固體潤滑膜時有助於增進二硫化鉬合基材的結合力，因此氮化鈦/二硫化鉬/金複合膜層之使用壽命可進一步獲得改善。

中文關鍵詞： 二硫化鉬、金、氮化鈦、固體潤滑膜、磨潤性質

英 文 摘 要 ： This study aims to enhance the endurance of MoS2 coating by applying a thin layer of Au (~0 nm) on MoS2 surface. Experimental results show that the addition of Au film increases the endurance of MoS2/Au over equivalent coatings without Au. The friction coefficient rapidly decreases to a stable value ($\mu$~.045) after about 100 cycles sliding. After more than 15,000 cycles, the friction coefficient gradually increased to a second stable value ($\mu$~.15). An average endurance of over 50,000 cycles was measured in this case. The Au or Au－MoS2 composite layer can effectively prevent oxygen or moisture reaction with MoS2 and hence significantly increases the wear life.

英文關鍵詞：

**行政院國家科學委員會補助專題研究計畫** ■**成果報告**
□**期中進度報告**

# 二硫化鉬/金固體潤滑膜之磨潤特性研究

計畫類別：■個別型計畫　□整合型計畫
計畫編號：NSC 99-2221-E-216-004
執行期間：99 年 08 月 01 日至 100 年 09 月 30 日
執行機構及系所：中華大學機械工程學系

計畫主持人：簡錫新
共同主持人：馬廣仁
計畫參與人員：吳崧銓、劉時瑞

成果報告類型(依經費核定清單規定繳交):■精簡報告 □完整報告

本計畫除繳交成果報告外，另須繳交以下出國心得報告：
□赴國外出差或研習心得報告
□赴大陸地區出差或研習心得報告
■出席國際學術會議心得報告
□國際合作研究計畫國外研究報告
處理方式：除列管計畫及下列情形者外，得立即公開查詢
□涉及專利或其他智慧財產權，□一年□二年後可公開　查詢

中　華　民　國　100　年　10 月　31　日

# 行政院國家科學委員會專題研究計畫成果報告

# 二硫化鉬/金固體潤滑膜之磨潤特性研究

The Study of Tribological Properties of MoS2/Au Solid Lubricant Coatings

計畫編號：NSC 99-2221-E-216-004

執行期限：99 年 08 月 01 日至 100 年 09 月 30 日

主持人：簡錫新 中華大學機械系

共同主持人：馬廣仁 中華大學機械系

計畫參與人員：吳崧銓、劉時瑞 中華大學機械系

**摘要**

本研究將嘗試在二硫化鉬薄膜上鍍很薄的金膜層(約 80 nm)來增進二硫化鉬薄膜之使用其壽命。研究結果顯示很薄的金膜在最外層，做磨耗試驗時觀察經過 100 道次的迴轉磨耗測試後，摩擦係數開始降低最後降低到一個穩定植（μ=0.045），經過 15000 道次的迴轉磨耗測試後，摩擦係數開始上升至第二個穩定植（μ=0.15）。膜層的壽命超過 50000 道次。證明金膜層或二硫化鉬/金複合膜層能有效防止了氧氣或濕氣與二硫化鉬發生反映，因此使二硫化鉬之使用壽命也因此大幅提升。

關鍵字：二硫化鉬、金、氮化鈦、固體潤滑膜、磨潤性質

**Abstract**

This study aims to enhance the endurance of $MoS_2$ coating by applying a thin layer of Au (~80 nm) on $MoS_2$ surface. Experimental results show that the addition of Au film increases the endurance of $MoS_2$/Au over equivalent coatings without Au. The friction coefficient rapidly decreases to a stable value (μ~= 0.045) after about 100 cycles sliding. After more than 15,000 cycles, the friction coefficient gradually increased to a second stable value (μ~= 0.15). An average endurance of over 50,000 cycles was measured in this case. The Au or Au–$MoS_2$ composite layer can effectively prevent oxygen or moisture reaction with $MoS_2$ and hence significantly increases the wear life.

## 一 背景說明

$MoS_2$ 固體潤滑膜的發展已逾 50 年，其在真空環境(如太空中)的潤滑扮演著無可取代的地位。$MoS_2$ 的潤滑機構中已有許多的研究報導，一般相信基面(Base plane)上

的 S 與 Mo 呈共價鍵結合，但層與層間則是以微弱的凡得瓦爾力結合；所以受剪力時 $MoS_2$ 很容易沿著基面間滑動，導致低摩擦係數 [1-3]。

$MoS_2$ 固體潤滑膜最大的隱憂是其潤滑性質對溼氣或氧氣氛十分敏感。通常氧原子易擴散進入 $MoS_2$，層與層的間隙易生成 MoOx，此一氧化反應破壞了原本層與層間微弱的凡得瓦爾力鍵結，導致喪失潤滑效果。一般在真空下，摩擦係數可達 0.01；但當相對溼度超過 50%時，摩擦係數可能高達 0.1，磨損壽命也隨著迅速降低 [3-6]。有鑑於此，此類薄膜常被限制於真空或者是相對濕度較低的氣氛下使用以確保其薄膜特性的應用。現今已經有許多產業逐漸重視這方面的問題，為此投入大量的研究成本，試圖拓展此系列固體潤滑膜之環境適應性來取代傳統思維的潤滑機制。

1980 年代濺鍍技術開始應用於沈積 $MoS_2$ 薄膜，雖然與基材間的結合力改善了，但緻密性仍然不理想。一直到了 1990 年代，磁控濺鍍技術發展後，由於離子電流密度及能量的提高，已使得 $MoS_2$ 薄膜的緻密性大為改善 [7,8]。Donnet 等人[8]在超真空下濺鍍沈積 $MoS_2$ 薄膜並在高真空下測得摩擦係數可低至 0.001，也證明了超真空下有利 $MoS_2$ 薄膜成長時基面平行於基材成長，因而有助於超低的摩擦係數。但是極高真空的濺鍍設備十分昂貴及耗時甚長，並不符合經濟效益。近來許多人嘗試在濺鍍 $MoS_2$ 的同時滲入金屬元素，以增進摩擦磨損性能(可由製作 $MoS_2$-金屬複合物靶材或同時濺鍍金屬與 $MoS_2$ 靶材達到目的)。

與一般 $MoS_2$ 固體潤滑薄膜相較下，$MoS_2$-Ti (MoST)硬度高、抗磨耗性佳而且對於大氣環境的適應性明顯優於 $MoS_2$ 膜層，因此 $MoS_2$-Ti (MoST)薄膜其良好的磨潤成效為相關產業界提供了更寬廣的應用[9]。近三年來已有相關報導證實二硫化鉬薄膜已成功的應用在各種刀具、模具及引擎上，此一結果使得 $MoS_2$ 薄膜的應用邁入新的里程(使用環境不再受限於高真空或開放環境)。

一般相信添加合金元素，可抑制鉬與氧發生氧化反應；另一可能的原因是金屬元素有利生成組織較緻密且基面平行基材的 $MoS_2$ 薄膜，因此降低了氧的擴散機會；然而真實的高濕度下低摩擦機構仍待進一步的釐清。本研究提出在二硫化鉬薄膜上鍍很薄的金膜層(約 80 nm)來改善 $MoS_2$ 薄膜之使用壽命，並探討其磨潤機制。

## 二 研究方法

本研究將以直流濺射法製作 $MoS_2$ 薄膜並尋求最佳之製程參數以利探討其磨潤性質。除此之外，探討 Au 薄膜鍍於 $MoS_2$ 薄膜表面對其磨潤性質所產生的影響。薄膜磨潤性質的測試則以 pin-on-disc 的方式進行，並經由側向力的量測獲得其摩擦係數。$MoS_2$ 薄膜顯微組織及磨耗機制將藉由 X 光線繞射儀高解析掃描式電子顯微

鏡分析探討。

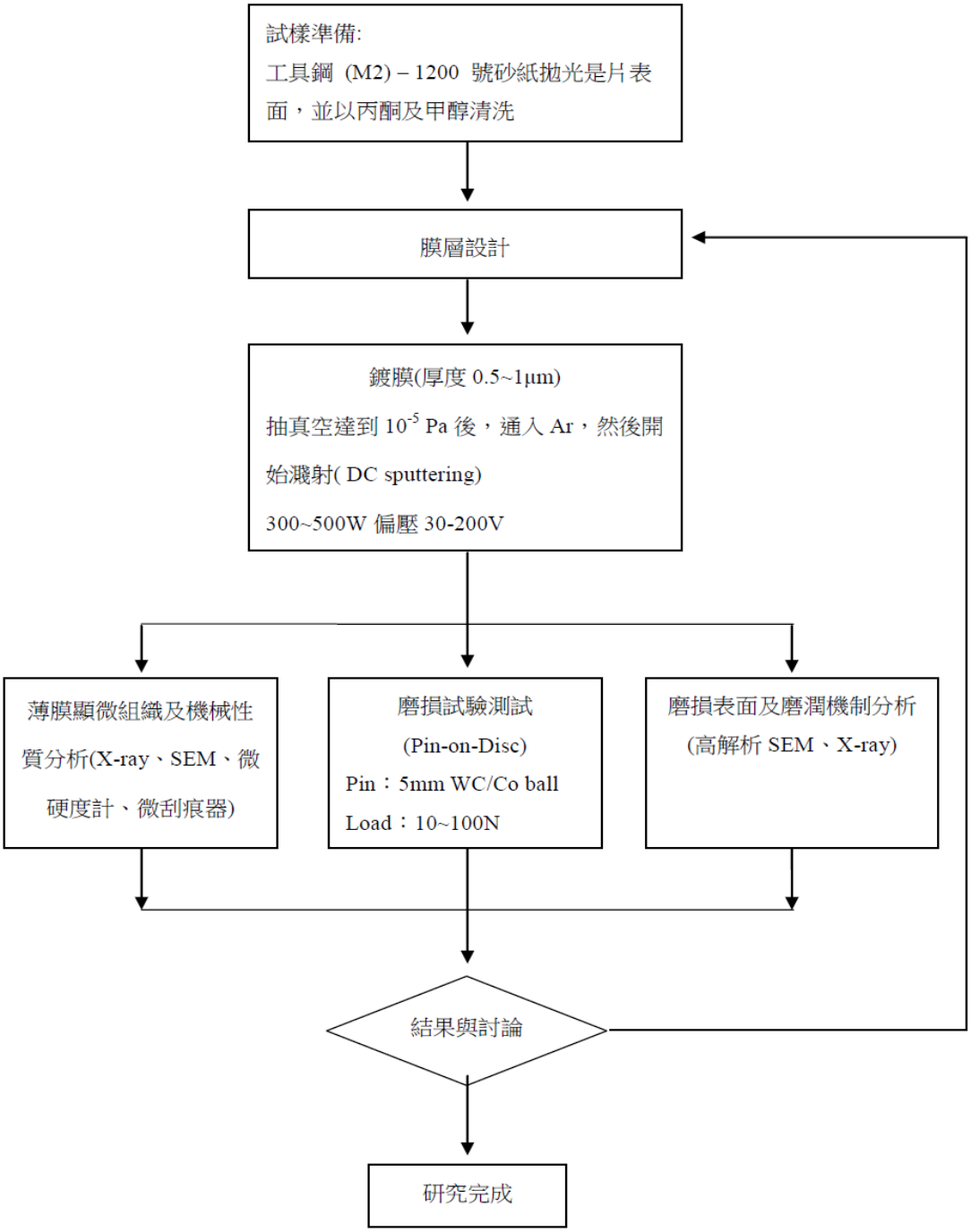
試樣準備:
工具鋼 (M2) – 1200 號砂紙拋光是片表面，並以丙酮及甲醇清洗
膜層設計
鍍膜(厚度 0.5~1μm)
抽真空達到 10-5 Pa 後，通入 Ar，然後開始濺射( DC sputtering)
300~500W 偏壓 30-200V
薄膜顯微組織及機械性質分析(X-ray、SEM、微硬度計、微刮痕器)
磨損試驗測試
(Pin-on-Disc)
Pin：5mm WC/Co ball
Load：10~100N
磨損表面及磨潤機制分析
(高解析 SEM、X-ray)
結果與討論
研究完成

## 三 結果與討論

### 微結構及機械性質

以磁控濺鍍法產生之$MoS_2$薄膜呈現緻密的柱狀組織，X 光結構分析呈現非晶態或奈米結晶特性(圖一)。二硫化鉬薄膜上鍍很薄的金膜層(約 80 nm)來增進二硫化鉬薄膜之使用其壽命。Mo:S 的化學組成比和製程參數有關，約為 1.4-1.6。微量的氧（<5%）被偵測到在鍍膜時摻雜進入 $MoS_2$ 膜層。以奈米壓痕器測得 $MoS_2$ 膜層的硬度為 5.20 GPa，彈性摩數為 102 GPa，顯示其硬度遠高於傳統的 $MoS_2$ 膜層。$MoS_2$ 以及 $MoS_2$/Au 膜層與基材的黏著強度超過 80 牛頓。圖二顯示在做硬度測試時層狀的結構非常容易在 $MoS_2$/Au 膜層上方生成。$MoS_2$ 膜層具有高硬度可歸因於其具有緻密的顯微組織。在刮痕及磨耗實驗測試時非晶態結構的 $MoS_2$ 膜層有很大的傾向生成層狀的結構。

### 磨潤性質

圖三比較添加了金膜在 $MoS_2$ 表面經過磨耗試驗後的結果。純的 $MoS_2$ 膜層具有很低的磨擦係數（μ=0.03）。然而，在經過了 9000 道次的迴轉磨耗測試後膜層失效，我們相信在剛開始測試時 $MoS_2$ 膜層生成層狀的結構使其具有低的摩擦係數，接著氧滲入層狀的 $MoS_2$ 膜層之間並發生氧化反應使其失效，在 $MoS_2$/Au 的雙層膜系統，摩擦係數起初接觸時很高（μ=0.15），顯示此時較高的磨擦係數主要由 Au 膜所主導，塑性流動主要發生在金膜層。重複的滑動使得金堆積在磨痕兩側使金膜層變簡薄。經過 100 道次的迴轉磨耗測試後，當剪應力滲透 $MoS_2$ 膜層並超過 $MoS_2$ 的剪力強度時，$MoS_2$ 膜層開始參與塑性流動過程，因此摩擦係數開始降低並達到一個穩定植（μ=0.045）。繼續滑動使得金膜和 $MoS_2$ 膜層形成很薄的 Au/$MoS_2$ 複合膜層。Au/$MoS_2$ 膜層有時會脫落並轉移至對面的磨球上，並黏附在底下的層狀 $MoS_2$ 的表面或破裂面的間隙內上，因此可有效的延遲氧和 $MoS_2$ 的反應。在這個階段塑性流動同時發生在 $MoS_2$ 膜層以及 Au/$MoS_2$ 複合膜層之間，因此摩擦係數或能量的損失較低，趨近如純的 $MoS_2$ 膜層。其關鍵在於 Au 膜不能太厚，這個結果和其他研究者做出來的結果有很大的不同，這也解釋了為何其他學者做出的結果摩擦係數較高的原因。研究也發現增加所施加的負荷，會有利於塑性流動較快的發生在 $MoS_2$ 膜層，因此可有利於降低摩擦係數。經過 15000 道次的滑動後整個 $MoS_2$ 膜層和金結合成 Au/$MoS_2$ 複合層，塑性流動主要發生在 Au/$MoS_2$ 複合膜層間，因此摩擦係數又升高到第二個穩定植，金的含量在經過 15000 道次的磨損後濃度為 10.30wt%，氧的濃度也隨著時

間而增加。相信 Au 或 Au/$MoS_2$ 複合膜層可有效的延遲氧或溼氣與 $MoS_2$ 膜層反應因此大大的增加了膜層的磨耗壽命，經過了 50000 道次的磨損試驗後，摩擦係數還能維持在 0.15，因此評估磨層的使用壽命超過 50000 道次。當減低金膜層厚度至 30 奈米可獲致較低的磨擦係數（0.04），但低磨擦係數只能夠維持到 11000 道次，摩擦係數就增加到較高的值（0.14-0.15）。估計的磨層使用壽命僅能達到 38000 道次。

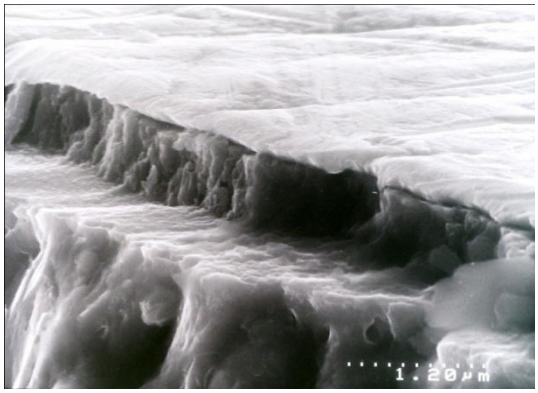


圖一　以非平衡磁控濺鍍設備製作出 $MoS_2$/Au 膜層之顯微組織。


圖二　顯示在做硬度測試後，在 MoS2/Au 膜層上方生成層狀的結構(荷重 300g) 。

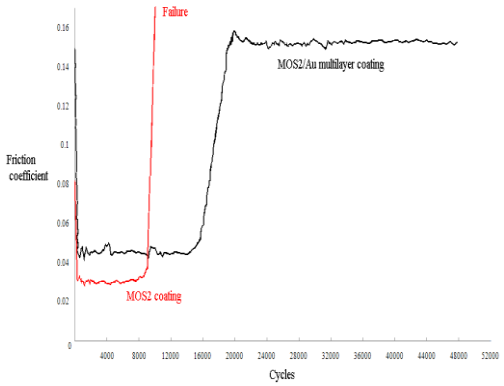


圖三　比較 MoS2 及 MoS2/Au 膜層之磨擦係數隨時間變化情形。

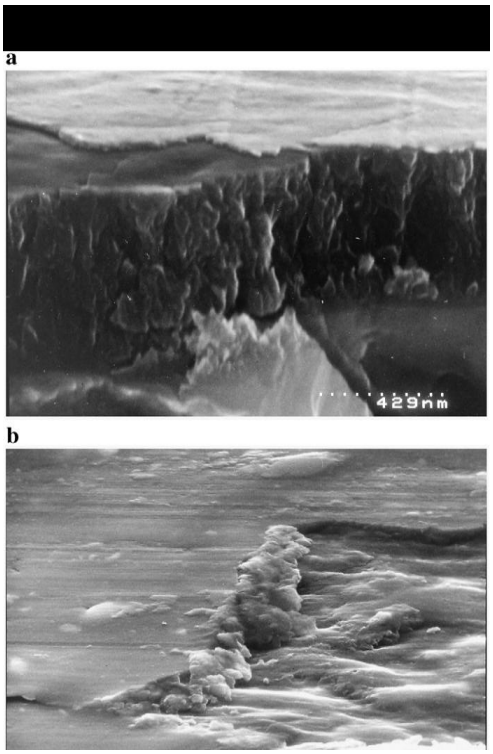


圖五　做磨耗試驗時應力傳遞到二硫化鉬膜層促使 MoS2 與 Au 在介面生成 MoS2-Au 複合膜層。

本研究中為進一步改善 $MoS_2$ 固體潤滑膜與基材的黏著強度，將先以磁控濺鍍

法在工具鋼基材上施鍍 TiN 膜層，藉由製程參數之控制，使其表面具有較疏鬆之柱狀晶結構，接續再共鍍 TiN 及 $MoS_2$-Ti (MoST) 膜形成漸進層，使 MoST 有機會在成膜時滲入 TiN 之柱狀晶粒之間，以增進 TiN 薄膜與 MoST 膜之間之結合強度，接續鍍 MoST 膜層，以利低摩擦係數 (圖六、七)。TiN 之柱狀晶結構有較有利於擄獲 MoST 的或 MoST-Au 磨屑，延續其潤滑功能。Au 膜層最後鍍在 MoST 的表面形成 TiN/MoST/Au 多層結構可改善氧化現象，以增進使用壽命 (圖八)。

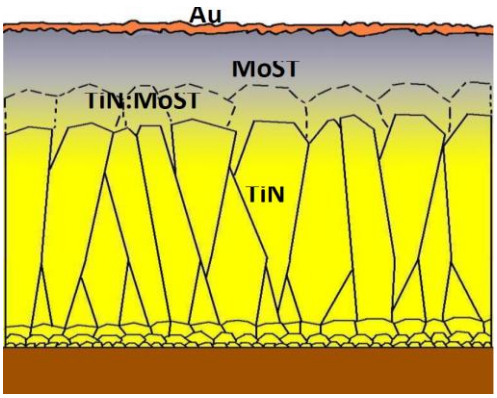


圖六 TiN/MoST/Au 多層結構示意圖。

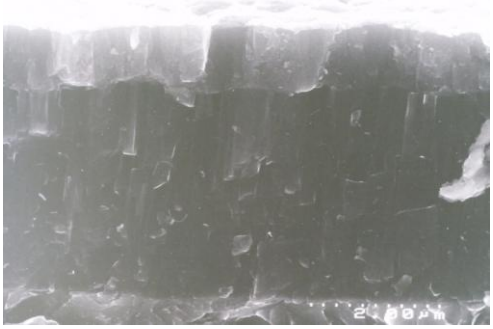

圖七 TiN/MoST/Au 多層結構顯織。

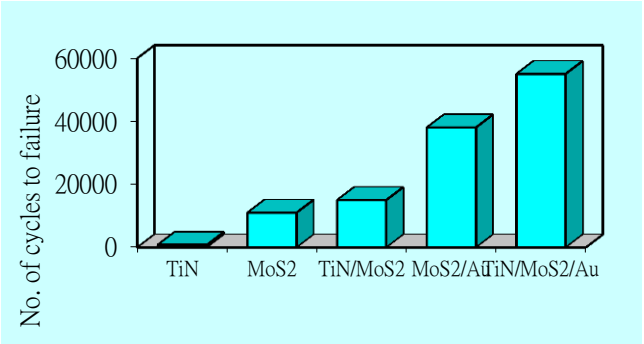


圖八 比較不同膜層之使用壽命。

## 四 結論

很薄的金膜在最外層，做磨耗試驗時應力傳遞到二硫化鉬膜層，使得非晶態二硫化鉬轉變為層狀二硫化鉬，因此具有極低的摩擦係數，因為金的存在可改善二硫化鉬氧化現象，因此長時間的磨耗試驗仍可使二硫化鉬/金複合膜層維持很低的摩擦係數，二硫化鉬之使用壽命也因此大幅提升。

## 五 參考文獻


1. J. C. Tyler and P. M. Ku, “Fundamental Investigation of Molybdenum Disulfide As a Solid Lubricant”, Final Technical Report, Contract No. w 66-0495-d, Naval Air Systems, Command, Washington, D.C., 1967.
2. J. T.cuum Spalvins, Vacuum Sci. Technol. A., vol. 5( 2), p. 212-219, 1987
3. E. F. Finkin, “Theory for the Friction of Sulfide and Other Thin Films”, Wear, vol. 18, p. 231, 1971.
4. I. L. Singer, “Solid Lubrication

Process", Fundamental of Friction: Macroscopic and Microscopic Process, Singer, I. L and Pollock, H. M. (Eds), Kluwer, 1992.

5. E. W. Robert and W. B. Price, "An Vacuum, Tribological Properties of High Rate Sputtered MoS2 Applied to Metal and Ceramic Substrates", New Materials Approaches to Tribology: Theory and Applications, Pope, L., Fehrenbacher, L. and Winer, W. (Eds), MRS Symposium, vol. 140, p. 251, 1989.
6. T. Spalvins, "Rreview of Recent Advances in Solid Film Lubrication", J. Vac. Sci. Technol., vol. A5(2), p. 212, 1987.
7. K. J. Ma, A. Bloyce, K. Mao., T. Bell and D. G. Teer, "Friction and Wear Behaviour of TiN/Au, TiN/MoS2, and TiN/TiCN/DLC Coatings", Presented at ICMCTF, 1996.
8. C. Donnet, M. Belin, T. LeMogne and J. M. Martin, "Tribological Behaviour of Solid Lubricated Contacts in Air and High-Vacuum Environment", The Third Body Concept, Dowson, D. et al (Eds), Elsevier, p. 389, 1996.
9. N. M. Renevier, V. C. Fox, D. G. Teer, J. Hampshire, "Performance of low friction $MoS_2$ titanium composite coatings used in forming applications", Materials and Design, vol. 21, p. 337-343, 2000.

# 出席國際學術會議心得報告Ⅰ

| | |
|---|---|
| 計畫編號 | NSC 99-2221-E-216-004 |
| 計畫名稱 | 二硫化鉬/金固體潤滑膜之磨潤特性研究 |
| 出國人員姓名<br>服務機關及職稱 | 馬廣仁　　中華大學機械系副教授 |
| 會議時間地點 | May 28-30, 2011, Changsha, China |
| 會議名稱 | 2011 International Conference on Chemical Engineering and Advanced Materials |
| 發表論文題目 | Microstructure and Mechanical Properties of Air Core Polymer Photonic Crystal Fibers |

一、參加會議經過

1. 國際化學及尖端材料工程會議主題涵蓋範圍很廣，主要有基礎化學工程、化學工程的應用及尖端材料工程三大部分。基礎化學工程部分有許多發表重點都在奈米複合材料的合成，包括碳纖維及無機氧化物纖維複材之製程及其性質探討等，少數文章討論環境及金屬回收之化工製程，議題較雜。化學工程的應用部分大部分著重能源、生醫及環境之應用，少數文章探討了鋁合金及銅合金之化學表面處理技術在 3C 產品之應用也受到廣大的迴響。尖端材料工程的議題很廣，較受注意的題目則在燃料電池材料及新型薄膜太陽能電池材料。有機薄膜太陽能電池材料雖然效能仍嫌不足，但製程較簡單且價格低廉，極有可能最後勝出。
2. 國際化學及尖端材料工程會議十分盛大，共有兩百多人與會，許多是世界知名學者，中國科學院相關領域的院士有兩位與會。作者發表之論文有關光子晶體光纖之製作及機械性質研究，係本計畫延伸出的結果，由於極具生醫及環境感測應用潛力，會後有許多學者詢問相關技術。目前中國大陸也有學者進行光子晶體光纖製作相關研究，但都同樣受限在資源不足，無法製作出高品質之光子晶體光纖，其他相關的光纖藕合問題也亟待解決。

二、與會心得

今年參加之會議都有意外之收獲，由於會議主題較廣，也較有工業應用價值，聽眾提的問題提供了不同的思考方向，對未來研究方向有極大的幫助。大會安排之參觀活動十分精采，也藉此機會認識相關之學者及瞭解其研究能量。由於會議主題太廣，較無法聚焦，對於議題深度之探討較嫌不足。

三、考察參觀活動(無是項活動者略)

四、建議

五、攜回資料名稱及內容

1.研討會參考資料

六、其他

# Microstructure and Mechanical Properties of Air Core Polymer Photonic Crystal Fibers

Hsi-Hsin Chien [1,2,a], Kung-Jeng Ma[1,2,b], Yun-Peng Yeh[1,c], and Choung-Lii Chao[3d]

[1]College of Engineering, Chung Hua University, No. 707, Sec. 2, Wu Fu Rd., Hsin Chu, Taiwan 30067.
[2]Department of Mechanical Engineering, Chung Hua University, No. 707, Sec. 2, Wu Fu Rd., Hsin Chu, Taiwan 30067.
[3]Department of Mechanical and Electro-Mechanical Engineering, Tam-Kang University, No.151 Ying-Chuan Road, Tamsui, Taipei Hsien, Taiwan 251.

[a]hhchien@chu.edu.tw, ma600229@ms17.hinet.net, [c]ivy639@yam.com, [d]clchao@mail.tku.edu.tw

**Keywords:** PMMA, air core, photonic crystal fibers, mechanical properties

**Abstract.** Polymer based photonic crystal fibers with low cost manufacturability, and the mechanical and chemical flexibility offer key advantages over traditional silica based photonic crystal fibers. PMMA photonic crystal fiber was fabricated by stacking an array of PMMA capillaries to form a preform, and followed by fusing and drawing into fiber with a draw tower. The air hole diameter and fraction of photonic crystal fiber can be manipulated by the thickness of PMMA capillaries and drawing temperature. The measurement of mechanical properties was performed by universal testing machine. The air core guiding phenomena was observed in air-core PMMA photonic crystal fiber. The ultimate tensile strength of PMMA photonic crystal fiber increases with the increase of the air-hole fraction. The mechanical strengths of all the microstructured optical fibers are higher than those of traditional PMMA fibers. This can be attributed to the introduction of more cellular interfaces which hinder the crack propagation and hence improve the mechanical strength. The plastic extension of PMMA microstructured optical fiber decreases with the increase of the air-hole fraction. Overall, the mechanical flexibility of PMMA microstructured optical fiber is superior than that of traditional PMMA optical fibers.

## Introduction

The silica-based air-guided photonic bandgap fibers have been developed recently [1-5]. The potential benefits of guiding light in air derive from lower Rayleigh scattering, lower nonlinearity and lower transmission loss compared to conventional waveguides. The polymer-based photonic bandgap fibers with low-cost manufacturability and the mechanical flexibility offer key advantages over conventional silica based photonic bandgap fibers. However, the fabrication of polymer photonic band gap fibers is more complicated due to the existence of severe water absorption, shrinkage, and poor thermal conductivities of polymer materials. Recently, solid core polymer PCFs, which are generally called microstructured optical polymer fibers (MPOFs), have been fabricated and studied [6]. However, the fabrication of air-guided polymer PCFs are still unsuccessful. The studies regarding their mechanical properties of polymer based PCF are still lacking.

In this work, we report the investigations of the parameters that are critical in the fabrication processes of air-core polymer photonic crystal fibers. The optical and mechanical properties of the air core PCFs are also investigated.

## Experimental

The fabrication processes of the air core polymer PCFs preform are illustrated in Figure 1. Hollow PMMA tubes (n~1.492) with 10 mm outer diameter and 8 mm inner diameter were first stacked into a hexagonal array. Some hollow tube(s) was/were removed at center site(s) in order to form the air core. The stacked tubes were annealed at 110 ℃ for 3 hours for water removal and then heated to form the preform. The drawing of the air-guided polymer PCFs is a two-step process. During the first step, the preform was drawn at an elevated temperature into a smaller preform with 40 cm in length and 10 mm in diameter. This smaller preform was then drawn again into a fiber with a diameter between 125 and 300 μm depending on the drawing temperature and speed. The drawing speed is controlled under 10 cm/min. From the stacked tubes to a fiber, the overall scale of the structure is reduced by a factor of 300, while the structure formed in the preform stage is still maintained. The measurement of mechanical properties was performed by universal testing machine. The loading foce is less than 5 kg and the loading speed is set at 5.2 mm/min. The resolution of the load cell approaches 0.5%.

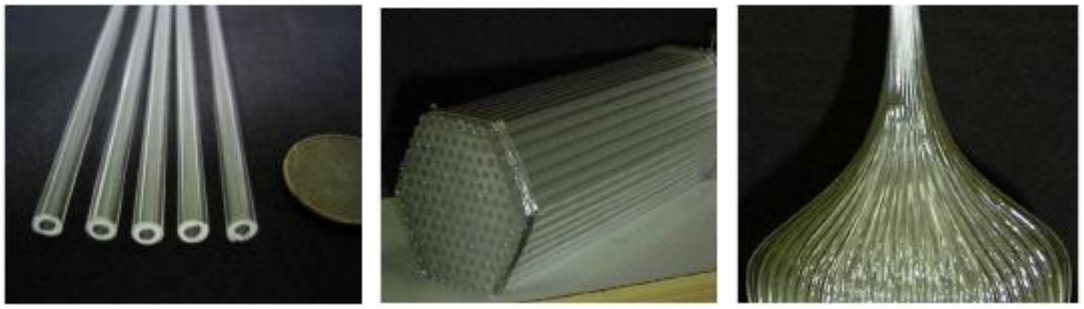

(a) (b) (c)

Figure 1. Fabrication processes of MPOFs. (a) step 1: cutting PMMA tubes; (b) step 2: packing and thermal annealing; (c) step 3: drawing into preform.

## Results and Discussion

The furnace temperature affects the formation of the air-guided polymer PCFs preforms. Uneven temperature distribution results in structure distortion or irregular hole diameters (Figure 2). The diameters of the air holes at the perimeter are smaller than those of the air holes near the center, which can be attributed to the significant thermal insulating effect in the polymer PCFs preform. The periphery of the preform will reach drawing temperature before the center does. Higher temperature leads to higher surface tension and thus larger air hole shrinkage. The larger the MPOF preform, the longer time is needed to achieve uniform temperature distribution over the whole sample. In fact, the diffusion treatment can be used to control the air hole diameter and air filling fraction.

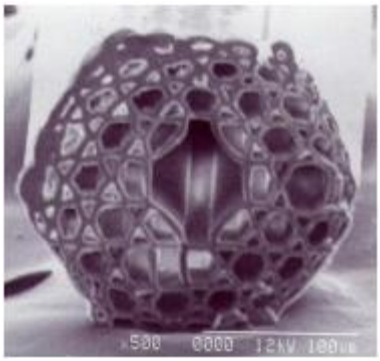

Figure 2. Drawing without enough diffusion treatment leads to irregular hole diameters.

The holding and fastening methods are also critical for the fabrication of high quality PCFs. The

holes structure has to be kept without block in order to remain gas flow and temperature distribution under steady state. The blocking in the air core during the drawing process will result in the expansion and distortion of the air core, as shown in Figure 3.

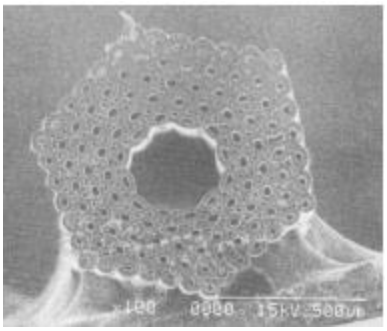

Figure 3. Drawing with block in the air core on the top of the PCFs perform results in the expansion and distortion of the air core.

The effects of drawing temperature were studied in detail. Drawing at temperature of 150℃ leads to the air-cored PCFs with air fraction higher than 80%, as shown in Figure 4(a). At the drawing temperature between 165 to 175℃, the ratio of the air hole diameter *d* to the pitch Λ between the holes remains almost the same. The small triangular air holes in the figures are the air gaps formed at corners of the stacked capillaries. The diameter *d* is in the range between 8 and 10μm, the pitch Λ is between 12 and 14 μm, and the fraction of air present in the samples is up to around 48% (Figure 4(b)). By increasing the furnace temperature to over 175℃, the triangular interstitial air holes become circular holes and the size of those holes is also reduced (Figure 4(c)). The maximum attainable air filling fraction is limited by the effect of surface tension. With this limitation, it is difficult to fabricate large air fraction samples with the small pitches.

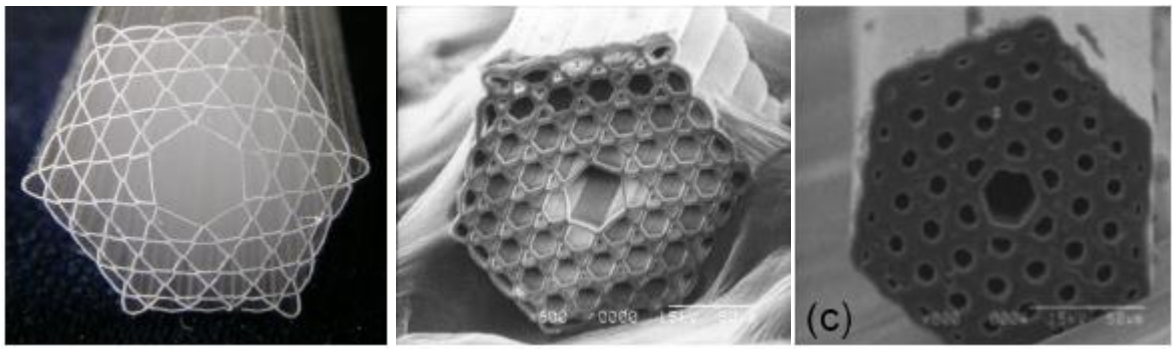


Figure 4 SEM images of the cleaved end-face of the MPOFs drawn at various temperature (a) 155℃ (b) 175℃ (c) 195℃.

The optical tests showed that air core PMMA photonic crystal fiber could well guide optical signals at wavelength of 632.8 nm. with air fraction above 48% (Figure 5). However the air-guiding phenomena disappears after 2 months possibly due to the absorption problems.

Figure 5. Measurement results of the MPOF samples. The air core PMMA photonic crystal fiber could well guide optical signals at wavelength of 632.8 nm. The sample was drawn at 175°C, with 1.5-hour diffusion treatment.

The yield strength and ultimate tensile strength and of air cored PMMA PCFs increases with the decrease of the drawing temperature (or with the increase of the air-hole fraction), as shown in Figure 6. The mechanical strengths of all the air cored PMMA PCFs are higher than those of traditional PMMA fibers. This can be attributed to the introduction of more cellular interfaces which hinder the crack propagation and hence improve the mechanical strength. The plastic extension of PMMA microstructured optical fiber decreases with the increase of the air-hole fraction, as shown in Figure 7. It is believed that the wall thickness of PMMA is helpful for the plastic extension of PCFs. It can be observed that the plastic extension of all the polymer PCFs is over 100%, which is higher than that of traditional PMMA fibers. It is interesting to note that the fractured surface demonstrates 45° cleavage facet rather than traditional ductile fractured surface (Figure 8). Further studies are needed for the investigation of the deformation and fracture mechanisms of polymer PCFs. Overall, the mechanical flexibility of PMMA air cored PCFs is superior than that of traditional PMMA optical fiber. This conclusion agrees with the results observed in cellular structured materials. The natural cellular structure such as woods, provides excellent deformation and energy adsorption capabilities [7]. The fabrication of polymer based PCFs provides a new route for the fabrication of biomimetic cellular materials and smart biosensors.

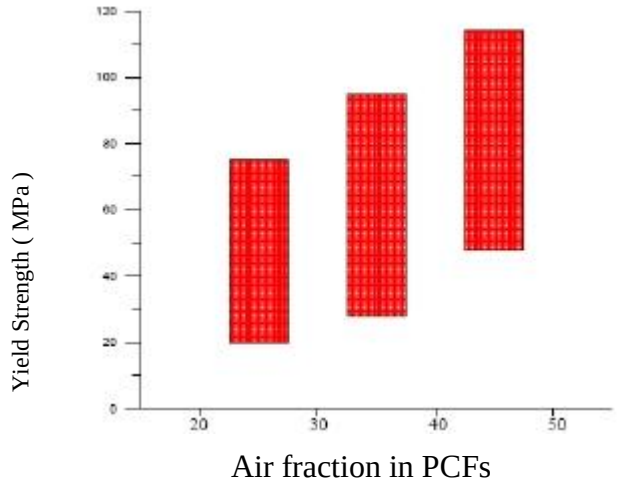


Figure 6. The influence of drawing temperature on the yield strength of air core polymer photonic crystal fibers.

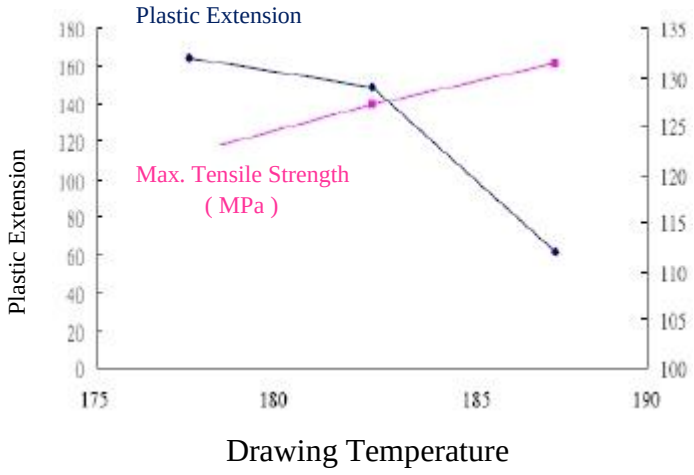


Figure 7. The influence of drawing temperature on the plastic extension of air core polymer photonic crystal fibers.

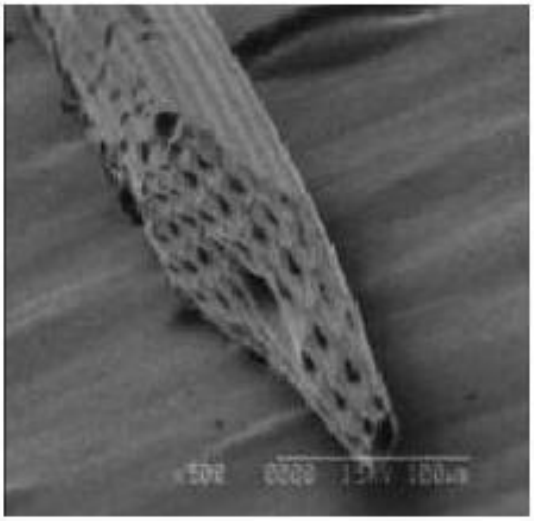

Figure 8. SEM image of fractured surface of polymer PCFs after tensile tests.

**Summary**

The air core guiding phenomena was observed in air-core PMMA photonic crystal fiber with air fraction above 48%. The ultimate tensile strength of PMMA photonic crystal fiber increases with the increase of the air-hole fraction. The mechanical strengths of all the microstructured optical fibers are higher than those of traditional PMMA fibers. This can be attributed to the introduction of more cellular interfaces which hinder the crack propagation and hence improve the mechanical strength. The plastic extension of PMMA microstructured optical fiber decreases with the increase of the air-hole fraction.

**Acknowledgements**

This research was supported by the National Science Council, The Republic of China, under Grant No. NSC 98-2221-E-216-010.

**References**

[1] J.C. Knight, J. Broeng, T. A. Birks and P.St.J. Russell: Science Vol. 282, (1998), p. 1476.

[2] R.F. Cregan, B. J. Mangan, J.C. Knight, T.A. Birks, P. St. J.Russell, P. J. Roberts, D. C. Allan: Science Vol. 285 (1999), p 1537.

[3] T.M. Monro, D.J. Richardson and P.J. Bennett: J. Lightwave Technol. Vol.17(6), (1999), p.1093.

[4] B. Temelkuran, S.D. Hart, G. Benoit, J.D. Joannopoulos and Y. Fink: Nature 420 (2002), p. 652.

[5] S.D. Hart, G.R. Maskaly, B.Temelkuran, P.H. Prideaux, J.D. Joannopoulos, and Y. Fink: Science, Vol. 296 (2002), p. 510.

[6] M.A. van Eijkelenborg, M.C. J. Large, A. Argyros, J. Zagari, S. Manos, N. A. Issa1, I. Bassett1, S. Fleming, R. C. McPhedran, C. de Sterke and N.A.P. Nicorovici: Optics Express Vol. 9 (2001), p. 319.

[7] L.J. Gibson andM.F. Ashby: Cellular Solids: Structure and Properties (Cambridge University Press U.K. 1999).

# 出席國際學術會議心得報告 II

| | |
|---|---|
| 計畫編號 | NSC 99-2221-E-216-004 |
| 計畫名稱 | 二硫化鉬/金固體潤滑膜之研究 |
| 出國人員姓名<br>服務機關及職稱 | 馬廣仁　中華大學機械系副教授 |
| 會議時間地點 | August 12 - 14, 2011　中國-哈爾濱 |
| 會議名稱 | 2011 International Conference on Electronic & Mechanical Engineering and Information Technology |
| 發表論文題目 | Kinetic Study of Bacterial Adhesion on Biomaterials by Using Optical Waveguide Lightmode Spectroscopy |

一、參加會議經過

此會議名稱為 IEEE 機電工程與資訊技術國際會議，會議地點設在哈爾濱理工大學。會議涵蓋的主題很廣，包含機電工程、機械設計製造及其自動化、先進材料與先進製造技術、機電工程、電腦軟體工程與資訊系統設計、電腦模擬與建模、電腦控制技術、計算科學及人工智慧等幾個大主題。共計 145 篇論文發表，參加人數逾 300 人。會議安排三個場地進行，並在會前安排了兩個半天的課程。第一天上午是由五位 IEEE 的 fellow 對最近發展較重要的議題作回顧，下午開始分場地不同主題發表論文。

作者較有興趣之主題為機械設計製造及其自動化，包括很多子題包含機械動力學及其應用、機械傳動理論及應用技術 、機械可靠性理論與工程、機械系統檢測技術、機械系統故障診斷與排除技術、摩擦磨損理論及應用、振動、雜訊分析與控制、機械結構動態分析、優化與控制、熱與熱傳導 、冶金新工藝、新技術、新方法、能源的儲運與開發、礦山機械設計與製造、新能源裝備製造、雲製造/極端製造、生物製造、現代集成製造技術、工業設計、工程優化、產品設計與開發、製造過程品質檢測與控制、電腦輔助設計、製造與工程 CAD/CAM/CAE 等。由發表的論文及聽眾看出來大家對機電整合技術及能源的應用課題較受矚目。新的太陽相關奈米材料也受到許多重視。大會還安排了廠商產品展示，及哈爾濱理工大學相關系所之研究成果展示。當然少不了大會安排的晚宴及參觀活動，由晚宴的安排可感受到東北人的熱情。

二、與會心得

大會安排了 keynote 講者及題目都是目前相關領域的一時之選，因此提問及討論都十分踴躍，由 keynote 演講內容很快的可以掌握目前該領域技術發展方向及困境。雖然個人對資訊及電腦運算主題不熟悉，但在講者的深入淺出的引導下也能很快進入狀況。個人較有興趣的題目是奈米材料及精密技術，也很幸運的聽到許多新的課題，對個人以後研發方向有許多啟發。此次會議我們發表之文章和生物感測及材料表面親疏水結構有關，未來可應用在生醫及民生產品，因此有許多學者主動和我們接觸，瞭解該技術之優勢及瓶頸。

三、考察參觀活動(無是項活動者略)

四、建議

哈爾濱一直是中國重工業發展重鎮，產學合作密切，此次會議也有機會認識幾位哈工大之教授，能充分了解哈爾濱機械產業發展方向及感受到哈爾濱傳統機械產業面臨轉型的壓力。由於本校已和哈爾濱理工學院互結姊妹校，此行所有教師都受到特別接待，盛情可感。我們也邀請機械學院的教師來本校參觀，並希望促成更多的學生來本校進行交換學生，做更多的學術交流。

五、攜回資料名稱及內容

1.研討會參考資料

六、其他

# *Kinetic Study of Bacterial Adhesion on Biomaterials by Using Optical Waveguide Lightmode Spectroscopy*

H.H. Chien[1,a], K.J. Ma[1,b], Jeremy J. Ramsden[2,c] and Y.P. Yeh[1,2,d]

[1] College of Engineering, Chung Hua University, HsinChu, Taiwan 300

[2] Cranfield University, Cranfield, Bedford, MK43 0AL England

[a]hhchien@chu.edu.tw, [b]kjma@chu.edu.tw, [c]j.ramsden@cranfield.ac.uk, [d]d09324003@chu.edu.tw

**Abstract.** The principles of bacterial identification are beginning to be understood at the kinetic level in the past few years, nevertheless, the crucial aspects to be taken into consideration are the spatial arrangements of molecules or atoms at the interacting surfaces and the profiles of the interfacial forces. In this study, the dynamics of attachment and detachment of *E.coli* K12 to ultra thin film silica and zirconia surfaces with precisely coated by sol-gel method is measured by using optical waveguide lightmode spectroscopy (OWLS) are described.

**Keywords:** bacterial adhesion, kinetic, optical waveguide lightmode spectroscopy

## I. **Introduction**

Bacterial adhesion to surfaces plays a major role in the transmission of pathogens, the persistent infection of surgical implants etc. There is therefore intense interest in designing surfaces to control (and hence eliminate, if deleterious) adhesion. There are indications that interaction energies determined by average physico-chemical properties of the bacterial and adsorbing surfaces play a determining rôle in adhesion [1]. The issue of identified bacteria to the unknown transmission of pathogens are important nowadays. Nevertheless, the traditional identification methods of bacteria are complex, expensive and time consuming, typically take 3 to 4 days, therefore, there is an intense interest in speeding up the determination of microbial pathogens. The natural environment of bacteria stay mostly at the interface of solid-liquid or solid-air interface and often freely float bacteria could be the first step of adhesion process, after bacteria arrive the surface, microbes tend to either attach to the surface or detach and return to their environment. Hence, it is crucial to understand bacterial adhesion tendence to surface. Bacterial adhesion to the surface has been studied in many previous works but many of them were focused on the specific adhesion molecules between bacteria and surface (e.g. Jucker, *et al.*(1997) [2] and Antonietta Splendiani, Cristiano Nicolella(2006) [3]); some of them were focused on the classification of gene expresion [4]. These techniques are slow, labor intensive and hence expensive. A more recent approach has been to use electrophoresis to separate bacteria on the basis of their surface electrostatic charge [5], which is not always a sufficiently good discriminator. The technique now widely called optical lightmode waveguide spectroscopy (OWLS) involves measuring the perturbation of the evanescent fields associated with one or more waveguide lightmodes [6]. It is particularly convenient to measure this perturbation with the help of a grating coupler [7], with which light can be coupled in or out of the waveguide. In this study, the adhesion kinetics of *E.coli* K12 and *L.plantarum* to $SiO_2$ and $ZrO_2$ are measured by using optical waveguide lightmode spectroscopy (OWLS) are demonstrated.

## II. Experimental

Optical Waveguide Lightmode Spectroscopy (OWLS) [8-9] is a label free technique for providing a high accuracy kinetic data required with excellent time resolution. This will enable us to probe hence understand the process involved in bacterial adhesion at nanometric precision. The changes of electronic polarizability in the measuring field of an optical waveguide alter the phase velocity of guided waves. This change can be interpreted as the change of mass and/or shape of adherent bacteria. A grating serves to incouple light into a planar optical waveguide in which the light then propagates, generating an evanescent field. The evanescent field is used to probe the optical properties of the solution in the vicinity of the surface. This method is based on its sensitivity to the changes of the refractive index when deposition of macromolecules occurs. This can be interpreted as the change of mass and/or shape of adherent bacteria.

The typical experimental situation to which the following procedure (see Figure 1) can advantageously be applied begins with a waveguide equilibrated with the medium used to suspend the bacteria, which are then (at time $t = 0$) flowed in suspension over the waveguide, leading to a gradual increase $b(t)$ in the number of adsorbed bacteria b per unit area until a steady state is reached at which $b(t)$ is constant, with a value of bsat. Usually pure suspending medium is then flowed over the waveguide to verify that the adsorption is irreversible. The quantity b is, to a good approximation, linearly proportional to an effective refractive index N of the waveguide, say the zeroth transverse electric (TE) one [10].

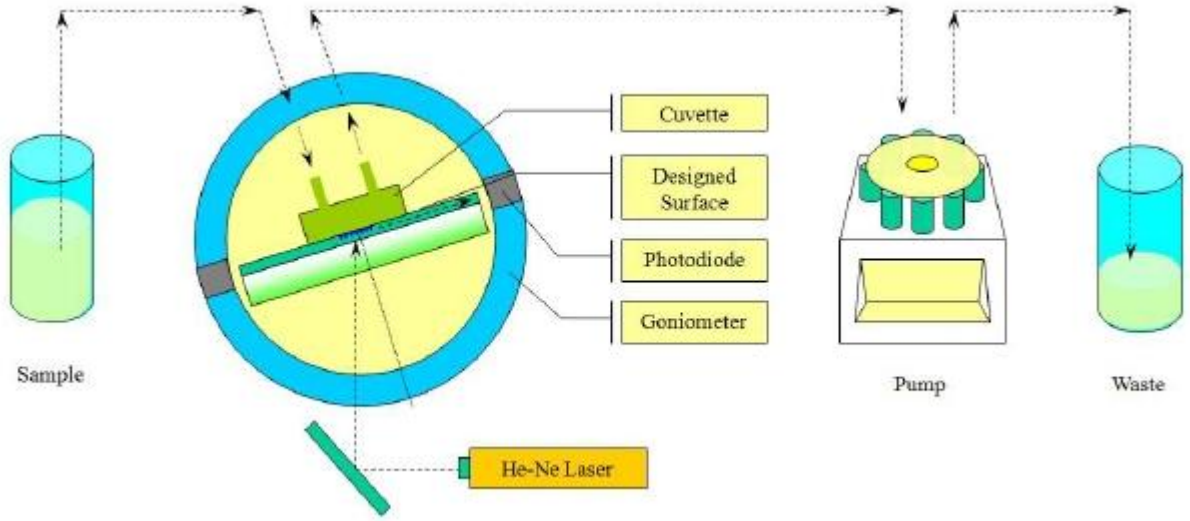


Figure 1. Typical experimental procedure for the kinetics of bacteria adhesion. Bacteria in PBS buffer solution was pumped through the optical waveguide lightmode spectroscopy by peristaltic pump. The flow rate is 10 μl/s and the temperature.

**Bacteria.** In this study, *Escherichia coli* (strain JM83, a K12 derivative) and *Lactobacillus plantarum* were chosen as they are common nonpathogenic strains and widely used for research, which makes them good representatives for investigating bacterial adsorption. A live sample of *E. coli* was cultured in 100 ml Luria broth (LB) overnight for approx. 18 hours at 37℃. *L. plantarum* was cultured in 100 ml MRS broth overnight at 30℃. Then the following step was the washing, hence, removing the traces of the liquid broth, which may interfere with the surface in the adsorption measurement. After supernatant removal, the pellets were resuspended in cold aqueous buffer, either PBS or Z 1150 buffer .

**Biomaterials.** The substrates for the bacterial adhesion in this experiment were biomaterial $SiO_2$ and $ZrO_2$, which was produced by physical vapour deposition (PVD) within the thickness 10 to 20 nm layer of silica and zirconia on glass weveguides gratings(ASI 2400, made by Microvacuum Ltd., Budapest, Hungary).

**Adsorption.** The investigation of adsorption kinetics is an extremely powerful and sensitive method for probing the energetic profile in the vicinity of an adsorbing surface. The kinetics of an interfacial reaction will be determined by the potential barriers experienced by the mobile component (bacteria were assumed to be a sphere of radius r) dissolved in a medium, as it approaches the stationary substrate. Normally, these barriers can be calculated by an adsorption rate coefficient $k_a$, where

$$k_a = \frac{D}{\delta_a} \tag{1}$$

where D is diffusion coefficient of bacteria and $\delta_a$ is adsorption distance which was given as [11]:

$$\delta_a = \int \left[ \exp\left( \frac{\Delta G_{123}(z)}{k_B T} \right) - 1 \right] dz$$

where $\Delta G_{123}$ is the interfacial free energy, $k_B$ is Boltzman constant ($1.38 \times 10^{-23}$ J/K) and T is absolute temperature.

The energy barrier can be presented by the adsorption rate of constant $k_a$ with

$$k_a \approx \omega \exp\left( \frac{-\Delta G_a}{k_B T} \right) \tag{3}$$

where ω is some intrinsic frequency factor and presume energy barrier is to be given by the unit of $k_B T$ . And the rate of adsorbed bacteria then can be written as:

$$\frac{db}{dt} = k_a (\Delta G_{123}) c_b \phi \tag{4}$$

where $c_b$ is the effective bulk concentration (include hydrodynamic function); b is number of bacteria per unit area; a is area occupied by one bacterium; ϕ is fraction of available adsorption surface, which is related to the size and shape of bacteria.

The typical experimental situation to which the following procedure can advantageously be applied begins with a waveguide equilibrated with the medium used to suspend the bacteria, which are then (at time t = 0) flowed in suspension over the waveguide, leading to a gradual increase b(t) in the number of adsorbed bacteria b per unit area until a steady state is reached at which b(t) is constant, with a value of bsat [12]. Usually pure suspending medium is then flowed over the waveguide to verify that the adsorption is irreversible.

## III. Results and Discussions

Figure 2 shows the results from a typical adsorption/desorption experiment. Adsorption approaches saturation, apparently asymptotically. Upon flooding with PBS buffer solution at the same flow rate, some bacteria were desorbed in this case. Note that the concentration of *E.coli* $c_b$=1.04x10$_8$ cells/ml and the concentration of *L.plantarum* $c_b$ = 4.22x10$_6$ cells/ml. $b_{sat}$ is read from the Figure 2 curve where the adsorption of bacteria reaches saturation.

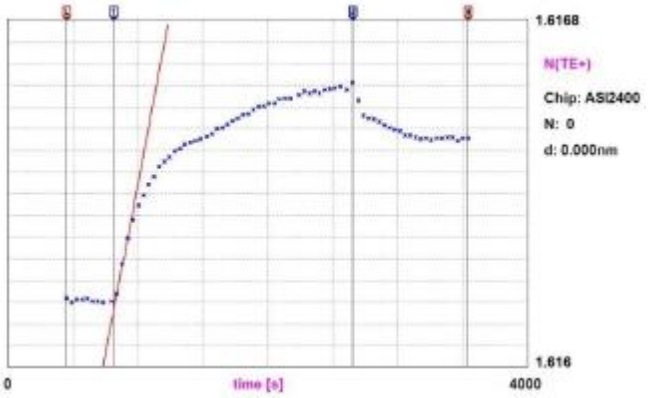


Figure 2. Typical raw OWLS result. Mark 1 indicates that the start of bacterial flow and Mark 2 indicates its end. The tangent shows the kinetic of the adsorption of *E.coli* K12.

For the adsorption objects to a surface, nevertheless, any kind of surface is mainly a continuum and it is known at once that the saturate surface "jammed" in the sense that there is no space to let objects move in, or there are very a lot of spare spaces but all the spare spaces may not be big enough separately to allow objects get in. For this problem of random sequential adsorption (RSA) to a surface has been noticed for a long time and the simplest process to solve the problem of loading up space by objects deposited sequentially at randomly chosen location in a continuous condition is random sequential addition (RSA) [6]. Figure 3 show the fitting results of the kinetics and mass of adsorbed bacteria on the surface. It is clear that a plot is reasonably well fitted by a random sequential adsorption process.

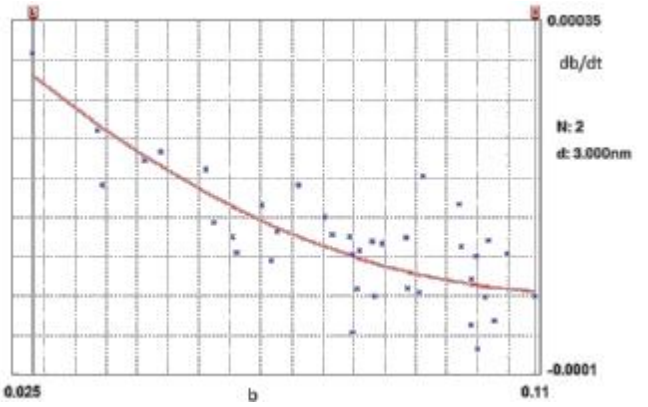


Figure 3. The result of the rate of the bacterial adsorption vs the number of bacteria on the surface with random sequential adsorption fit.

The adsorption results of *E.coli* on silica($SiO_2$) and zirconia($ZrO_2$) were shown in Table 1. Note that $k_a$ and a respectively are the kinetic rate coefficient of adsorption and the area occupied by one bacterium and both are derived from fitting Equation (4). The rate of adsorption and the area occupied by one bacterium of $ZrO_2$ are also higher than $SiO_2$. This indicates that $ZrO_2$ has a stronger force to attract *E.coli* than $SiO_2$. The measured interfacial free energy of *E.coli* on both surfaces are -6.8x10$^{-7}$ and -11.7x10$^{-7}$ mJm$^{-2}$ respectively.

**Table 1** The adsorption results of *E.coli* K12 on $SiO_2$ and $ZrO_2$.

| Adsorbent | $SiO_2$ | $ZrO_2$ |
|---|---|---|
| $b_{sat}/\mu m^{-2}$ | 0.11 | 0.105 |
| $k_a/\mu ms^{-1}$ | 0.23 | 0.46 |
| Measured Interfacial free energy($10^{-7}$) /mJm$^{-2}$ | -6.8 | -11.7 |
| a/$\mu m^2$ | 3.22 | 4.26 |

Table 2 shows the results of area occupied by one bacterium on both surface in phosphate (PBS) and chloride (Z1150) buffer solutions. Note that zirconia($ZrO_2$) has less area occupied by *L.plantarum*, which zirconia($ZrO_2$) has higher occupied area by *E.coli*. Also note that the chloride in buffer solution could alter the attachment of bacteria to different surfaces. On the other hand, the dependence on ion type - comparing PBS and Z1150 - on silica($SiO_2$), the difference is not so great (slightly smaller in PBS for both *E.coli* and *L.plantarum*). On zirconia($ZrO_2$), there is a dramatic difference - *E.coli* is bigger in PBS, but *L.plantarum* is smaller.

**Table 2** Area occupied by one bacterium(a/$\mu m_2$) in PBS (phosphate) and Z1150 (chloride).

| Adsorbent | $SiO_2$ | $ZrO_2$ |
|---|---|---|
| $b_{sat}/\mu m^{-2}$ | 0.11 | 0.105 |
| $k_a/\mu ms^{-1}$ | 0.23 | 0.46 |
| Measured Interfacial free energy($10^{-7}$) /mJm$^{-2}$ | -6.8 | -11.7 |

## IV. Conclusion

In this study, the adhesion kinetics results of *E.coli* K12 and *L.plantarum* to surface $SiO_2$ and $ZrO_2$ in PBS and Z1150 have been demonstrated by optical waveguide lightmode spectroscopy (OWLS). The interaction of two kinds of bacteria, which are gram-positive and gram-negative bacteria, can be well predicted and their interfacial energies are deducible from the adsorption kinetics in the experiment. Furthermore, the rate of adsorption is characterized by the adsorption rate constant $k_a$, is inversely proportional to the integral of the bacteria substrate interfacial free energy $\Delta G_{123}$.

Bacterial adsorption is complicated, however bacteria have a characteristic surface chemical signature which could selectively bind to surface. Bacterial adsorption also follows the role of random sequential adsorption, which that means not only should the kinetics follow the characteristic random sequential adsorption law, but if the adsorption is irreversible then a should be irrespective to the surface. Given, however, the experimental difficulties inherent in measurements of the adsorption of a living bacterium, the methodology presented in the work is likely to be adequate for many purposes, which might include further analysis of the adsorption kinetics and demonstrate bacterial and other biomaterials in the future.

## References


[1] H. C. van der Mei, B. van de Belt-Gritter, G. Reid, H. Bialkowska-Hobrzanska, and H. J. Busscher, "Adhesion of coagulase-negative staphylococci grouped according to physico-chemical surface properties," *Microbiology,* vol. 143, pp. 3861-3870, December 1, 1997 1997.

[2] B. A. Jucker, H. Harms, S. J. Hug, and A. J. B. Zehnder, "Adsorption of bacterial surface polysaccharides on mineral oxides is mediated by hydrogen bonds," *Colloids and Surfaces B: Biointerfaces,* vol. 9, pp. 331-343, 1997.

[3] A. G. L. Antonietta Splendiani, Cristiano Nicolella,, "Control of membrane-attached biofilms using surfactants," *Biotechnology and Bioengineering,* vol. 94, pp. 15-23, 2006.

[4] S. Vilain, P. Cosette, M. Hubert, C. Lange, G.-A. Junter, and T. Jouenne, "Proteomic analysis of agar gel-entrapped *Pseudomonas aeruginosa*," *PROTEOMICS,* vol. 4, pp. 1996-2004, 2004.

[5] W. S. Ramsey, E. D. Nowlan, and L. B. Simpson, "Resolution of microbial mixtures by free flow electrophoresis," *Applied Microbiology and Biotechnology,* vol. 9, pp. 217-226, 1980.

[6] J. J. Ramsden, "Review of new experimental techniques for investigating random sequential adsorption," *Journal of Statistical Physics,* vol. 73, pp. 853-877, 1993.

[7] K. Tiefenthaler and W. Lukosz, "Sensitivity of grating couplers as integrated-optical chemical sensors," *Journal of the Optical Society of America B,* vol. 6, pp. 209-220, 1989.

[8] I. Szendro, "Art and practice to emboss gratings into sol-gel waveguides," in *Functional Integration of Opto-Electro-Mechanical Devices and Systems*, San Jose, CA, USA, 2001, pp. 80-87.

[9] Vörös.J., J. J. Ramsden, G. Csúcs, I. Szendro, S. M. De Paul, M. Textor, and N. D. Spencer, "Optical grating coupler biosensors," *Biomaterials,* vol. 23, pp. 3699-3710, 2002.

[10] E. K. Mann, "Evaluating Optical Techniques for Determining Film Structure: Optical Invariants for Anisotropic Dielectric Thin Films," *Langmuir,* vol. 17, pp. 5872-5881, 2001.

[11] L. A. Spielman and S. K. Friedlander, "Role of the electrical double layer in particle deposition by convective diffusion," *Journal of Colloid and Interface Science,* vol. 46, pp. 22-31, 1974.

[12] Y.-P. Yeh and J. J. Ramsden, "Quantification of the number of adsorbed bacteria on an optical waveguide," *Journal of Biological Physics and Chemistry* vol. 10, pp. 53-54, 2010.

# 國科會補助計畫衍生研發成果推廣資料表

日期:2011/12/21

| 國科會補助計畫 | 計畫名稱: 二硫化鉬/金固體潤滑膜之磨潤特性研究 |
|---|---|
| | 計畫主持人: 簡錫新 |
| | 計畫編號: 99-2221-E-216-004- 學門領域: 加工與製造 |

無研發成果推廣資料

# 99 年度專題研究計畫研究成果彙整表

| 計畫主持人：簡錫新 | 計畫編號：99-2221-E-216-004- |
|---|---|
| 計畫名稱：二硫化鉬/金固體潤滑膜之磨潤特性研究 | |

| 成果項目 | | | 量化 | | | 單位 | 備註（質化說明：如數個計畫共同成果、成果列為該期刊之封面故事...等） |
|---|---|---|---|---|---|---|---|
| | | | 實際已達成數（被接受或已發表） | 預期總達成數(含實際已達成數) | 本計畫實際貢獻百分比 | | |
| 國內 | 論文著作 | 期刊論文 | 0 | 0 | 100% | 篇 | |
| | | 研究報告/技術報告 | 1 | 0 | 100% | | |
| | | 研討會論文 | 1 | 0 | 100% | | |
| | | 專書 | 0 | 0 | 100% | | |
| | 專利 | 申請中件數 | 0 | 0 | 100% | 件 | |
| | | 已獲得件數 | 0 | 0 | 100% | | |
| | 技術移轉 | 件數 | 0 | 0 | 100% | 件 | |
| | | 權利金 | 0 | 0 | 100% | 千元 | |
| | 參與計畫人力（本國籍） | 碩士生 | 2 | 0 | 100% | 人次 | |
| | | 博士生 | 0 | 0 | 100% | | |
| | | 博士後研究員 | 0 | 0 | 100% | | |
| | | 專任助理 | 0 | 0 | 100% | | |
| 國外 | 論文著作 | 期刊論文 | 1 | 0 | 100% | 篇 | |
| | | 研究報告/技術報告 | 0 | 0 | 100% | | |
| | | 研討會論文 | 0 | 0 | 100% | | |
| | | 專書 | 0 | 0 | 100% | 章/本 | |
| | 專利 | 申請中件數 | 0 | 0 | 100% | 件 | |
| | | 已獲得件數 | 0 | 0 | 100% | | |
| | 技術移轉 | 件數 | 0 | 0 | 100% | 件 | |
| | | 權利金 | 0 | 0 | 100% | 千元 | |
| | 參與計畫人力（外國籍） | 碩士生 | 0 | 0 | 100% | 人次 | |
| | | 博士生 | 0 | 0 | 100% | | |
| | | 博士後研究員 | 0 | 0 | 100% | | |
| | | 專任助理 | 0 | 0 | 100% | | |

| | |
|---|---|
| 其他成果<br>(無法以量化表達之成果如辦理學術活動、獲得獎項、重要國際合作、研究成果國際影響力及其他協助產業技術發展之具體效益事項等，請以文字敘述填列。) | 無 |

| | 成果項目 | 量化 | 名稱或內容性質簡述 |
|---|---|---|---|
| 科教處計畫加填項目 | 測驗工具(含質性與量性) | 0 | |
| | 課程/模組 | 0 | |
| | 電腦及網路系統或工具 | 0 | |
| | 教材 | 0 | |
| | 舉辦之活動/競賽 | 0 | |
| | 研討會/工作坊 | 0 | |
| | 電子報、網站 | 0 | |
| | 計畫成果推廣之參與（閱聽）人數 | 0 | |

# 國科會補助專題研究計畫成果報告自評表

請就研究內容與原計畫相符程度、達成預期目標情況、研究成果之學術或應用價值（簡要敘述成果所代表之意義、價值、影響或進一步發展之可能性）、是否適合在學術期刊發表或申請專利、主要發現或其他有關價值等，作一綜合評估。

1. 請就研究內容與原計畫相符程度、達成預期目標情況作一綜合評估

■達成目標

□未達成目標（請說明，以 100 字為限）

□實驗失敗

□因故實驗中斷

□其他原因

說明：

2. 研究成果在學術期刊發表或申請專利等情形：

論文：■已發表 □未發表之文稿 □撰寫中 □無

專利：□已獲得 □申請中 ■無

技轉：□已技轉 ■洽談中 □無

其他：(以 100 字為限)

3. 請依學術成就、技術創新、社會影響等方面，評估研究成果之學術或應用價值（簡要敘述成果所代表之意義、價值、影響或進一步發展之可能性）(以 500 字為限)

本研究證明金膜層或二硫化鉬/金複合膜層能有效防止了氧氣或濕氣與二硫化鉬發生反映，因此使二硫化鉬之使用壽命也因此大幅提升。研究成果對二硫化鉬固體潤滑膜之未來發展具重要意義，未來該膜層可用於高濕度之環境，可解決許多超低摩擦機構件之表面處理問題。目前已有國內廠商洽談技術細節及技術轉移之可能性。